International Journal of Solids and Structures 49 (2012) 527–536

Contents lists available at SciVerse ScienceDirect

International Journal of Solids and Structures

journal homepage: www.elsevier.com/locate/ijsolstr

Analysis of spherical indentation of materials with plastically graded surface layer

Fuping Yuan *, Ping Jiang, Jijia Xie, Xiaolei Wu

State Key Laboratory of Nonlinear Mechanics, Institute of Mechanics, Chinese Academy of Science, Beijing 100190, China

ARTICLE INFO

Article history:
Received 5 April 2011
Received in revised form 19 October 2011
Available online 25 October 2011

Keywords:
Spherical indentation
Plastically graded materials
Contact
Dimensional analysis
Finite element modeling

ABSTRACT

In the present work, a comprehensive parametric study for establishing contact mechanics of instrumented normal spherical indentation on homogeneous materials and materials with plastically graded surface layer (PGSL) was undertaken by dimensional analysis and finite element modeling. The spherical indentation response for homogeneous materials can be described only by two dimensionless parameters: strain hardening exponent and a unified parameter that can describe effects of both the normalized yield strength and the normalized indentation depth. The influences of these two parameters were investigated for a wide range of engineering materials, and the results may be used as an estimate of loading response and pile-up/sink-in behavior when the material properties are known. In the materials with PGSL, a linear gradient in yield strength, and no variation in elastic modulus and strain hardening exponent were explored. The indentation response of the materials with PGSL can be described only by three dimensionless parameters: the normalized indentation depth, the dimensionless strength gradient parameter, and the normalized PGSL thickness. The effects of these three parameters were studied systematically. The normalized pile-up/sink-in parameter is found to be an increasing function of the strength gradient parameter. The normalized pile-up/sink-in parameter increases (decreases) with increasing PGSL thickness for a fixed positive (negative) gradient case at large indentation depth. The results also indicate that the materials with positive PGSL can bear more loads and have significantly more resistance to contact crack formation.

1. Introduction

In nature, most failures of materials occur on their surfaces, such as fatigue fracture, wear and corrosion, fatigue and tribological damage (Roland et al., 2006). Thus, introduction of gradients in surface properties has been realized as a useful method for improving the mechanical performance of materials (Suresh and Mortensen, 1998; Suresh, 2001; Chen et al., 2005; Roland et al., 2007). Graded structures with gradients in microstructure and/or composition are commonly observed in natural and biological materials such as bamboos, shells, bones and teeth (Suresh and Mortensen, 1998). In engineering design, major methods for manufacturing graded surface layer include carburizing, nitriding, ion implantation, electro-deposition technique and surface severe plastic deformation method (Tartaglia and Eldis, 1984; Nastasi et al., 1998; Choi et al., 2008a; Tao et al., 2002; Waltz et al., 2009; Branch et al., 2011).

Instrumented normal indentation testing has been widely used as an attractive method of determining mechanical properties of materials and characterizing the mechanics of contact at material surfaces (Vanlandingham, 2003; Cheng et al., 2004; Gouldstone et al., 2007). However, the true contact area cannot be easily determined from indentation load-depth data because of pile-up/sink-in behavior around the contact surface (Bolshakov and Pharr, 1998). Unlike conical and pyramidal indenters, the pile-up/sink-in behavior of spherical indentation is a function of the indentation depth since the material is transited from elastic deformation at small depths to fully plastic deformation at large depths (Taljat and Pharr, 2004). Although the evolution of pile-up/sink-in behavior in the elastic–plastic transition for spherical indentation has been investigated in the literature (Biwa and Storakers, 1995; Kogut and Komvopoulos, 2004; Cao and Lu, 2004a; Taljat and Pharr, 2004; Lee et al., 2005; Habbab et al., 2006; Hernot et al., 2006; Kim et al., 2006; Bartier et al., 2010), a comprehensive parametric study for interpreting instrumented normal spherical indentation is still needed.

The early studies of contact indentation mechanics for materials with graded surface involved with elastic modulus gradients (Giannakopoulos and Suresh, 1997). These investigations indicated that elastic positive graded materials have significantly more resistance to Hertzian cone crack formation due to stress redistribution. The tensile stresses around the indenter contact perimeter can be redistributed to the stronger material beneath the surface. After these early studies, contact indentation mechanics with various indentation shapes for elastic graded materials has been well

* Corresponding author. Tel.: +86 01082544170; fax: +86 01082543977.
E-mail addresses: fpyuan@lnm.imech.ac.cn (F. Yuan), jping@imech.ac.cn (P. Jiang), xiejj@lnm.imech.ac.cn (J. Xie), xlwu@imech.ac.cn (X. Wu).

0020-7683/$ - see front matter © 2011 Elsevier Ltd. All rights reserved.
doi:10.1016/j.ijsolstr.2011.10.018

documented (Jitcharoen et al., 1998; Suresh and Mortensen, 1998; Suresh et al., 1999; Suresh, 2001), including both normal indentations and frictional sliding simulations.

Nakamura et al. (2000) first used an inverse analysis and instrumented micro-indentation to study plastically graded materials (PGM). Their procedure can be used to extract the important properties of the plastically graded layers, and is also applicable in estimating physical and mechanical properties of other layered materials. Later on, Cao and Lu (2004b) developed an analytical expression to predict the loading vs. indentation depth curve for PGM. They also developed a reverse algorithm to determine the plastic properties of a plastically graded surface. Giannakopoulos (2002) investigated the normal indentation of plastically graded substrates by sharp conical indenters. Their analysis enabled the direct correlation of the plastic properties and the load-penetration curves obtained from instrumented indentation tests, and their results showed that proper control of graded plastic property can strengthen substrates against contact induced damage. In the following work, Choi et al. (2008b) developed a comprehensive and quantitative mechanics framework for interpreting instrumented conical sharp indentation of plastically graded ductile metals. Although contact mechanics of PGM by sharp indenters has been well understood, a systematic understanding of mechanics of spherical indentation for PGM still needs further investigation. The elastic–plastic indentation of a half space by a rigid sphere is a fundamental problem in contact mechanics and of great importance in various applications such as gears, rollers, contact fatigue and fracture analysis of devices. Therefore, the objective of the present work is to develop a comprehensive parametric study for establishing contact mechanics of instrumented normal spherical indentation on homogeneous materials and materials with plastically graded surface layer (PGSL). In the first part of this paper, we establish a systematic methodology using dimensional analysis and FEM simulations to quantify various parameter effects on the normal spherical indentation response for homogeneous materials. In the second part of this work, a comprehensive understanding of normal spherical indentation on the materials with PGSL is presented.

2. Geometrical and computational model setup

2.1. Geometrical model

In the materials with PGSL, a linear gradient in yield strength (without variations in elastic properties and strain hardening exponent) is investigated as the first step to establish fundamental framework and the general trend. Such a graded material system is also common in nanocrystalline (NC) metals and alloys manufactured by a variety of methods (Meyers et al., 2006; Dao et al., 2007; Choi et al., 2008a). A gradient in yield strength can be introduced by variations in grain size, but without necessarily requiring a gradient in elastic properties. Moreover, the strain hardening exponent of NC metals is essentially zero over a broad range of achievable yield stresses, and then gradients in strain hardening exponent can be minimized as well. The underlying mechanics principles and computational procedure remain essentially the same, but more complicated for nonlinear gradients in yield strength and gradients in strain hardening exponent, which will be addressed in the future work. Fig. 1 shows the configuration of normal spherical indentation of materials with PGSL.

The PGSL and the underlying matrix material are modeled by Hooke's law and the von Mises yield criterion with isotropic power law hardening. Thus, the true stress σ and the true strain ε relationship under uniaxial strain condition can be expressed as

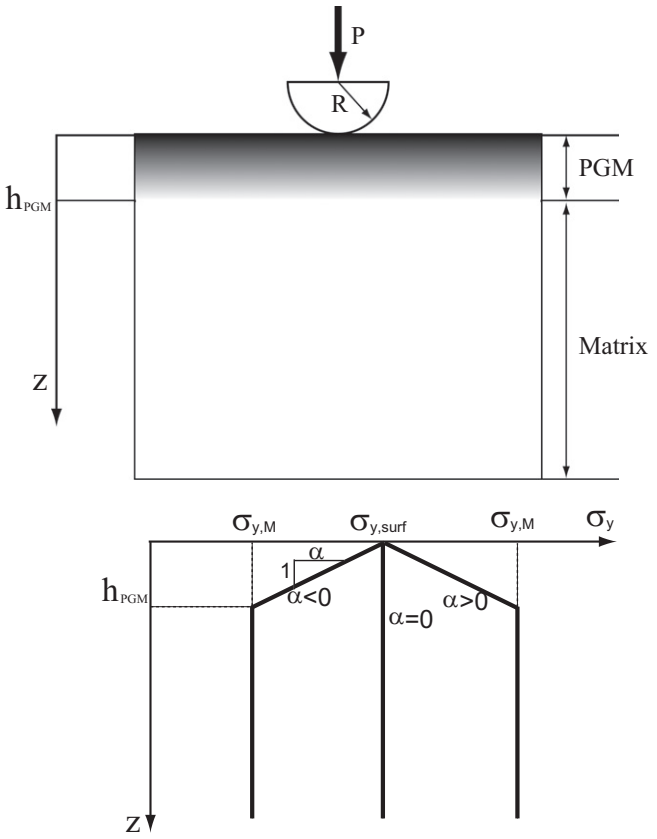

Fig. 1. Schematic diagram of materials with plastically graded surface layer under normal spherical indentation.

$$\begin{cases} \sigma = E\varepsilon, & \text{for } \sigma \leqslant \sigma_y \\ \sigma = C\varepsilon^n, & \text{for } \sigma \geqslant \sigma_y \end{cases} \tag{1}$$

where E is the Young's modulus, C is the strength coefficient, σ_y is the yield strength at zero plastic strain and n is the strain hardening exponent.

Decomposing the strain into the yield and the plastic strain, and applying the condition of continuity at yielding point for Eq. (1), the true stress-true strain equation can be rewritten as

$$\begin{cases} \sigma = E\varepsilon, & \text{for } \sigma \leqslant \sigma_y \\ \sigma = \sigma_y(1 + E\varepsilon_p/\sigma_y)^n, & \text{for } \sigma \geqslant \sigma_y \end{cases} \tag{2}$$

The linear gradient of yield strength in the plastically graded surface layer is defined as

$$\begin{cases} \sigma_y(z) = \sigma_{y,surf}(1 + \alpha z), & \text{when } 0 \leqslant z \leqslant h_{PGM} \\ \sigma_y(z) = \sigma_{y,M}, & \text{when } z \geqslant h_{PGM} \end{cases} \tag{3}$$

where z is the depth from the surface, $\sigma_{y,surf}$ is the yield strength at the surface, $\sigma_{y,M}$ is the yield strength of the matrix beneath the plastically graded layer, α is the parameter of gradient, and h_{PGM} is the thickness of plastically graded layer. For $\alpha = 0$, homogeneous material is recovered; while for $\alpha < 0$, the yield strength decreases with the depth; and for $\alpha > 0$, the yield strength increases with the depth.

2.2. Computational model

Simulation of the spherical indentation was performed using ABAQUS Theory Manual (v6.8) (2008). As shown in Fig. 2, an axisymmetric two-dimensional formulation was employed. The dimension of the substrate was set large enough to ignore the effect of boundary conditions. The spherical indenter was modeled

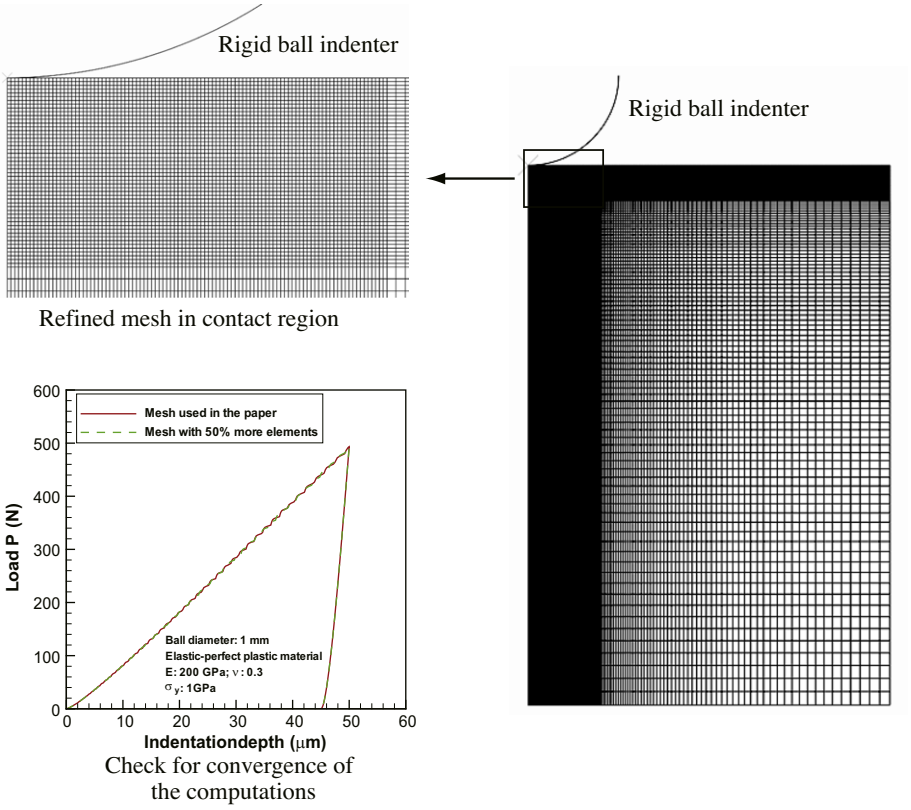

Fig. 2. Finite element mesh used for the normal spherical indentation and convergence check for the computations.

as a rigid sphere with a diameter of 1 mm, and the semi-infinite substrate was modeled using 20800 four-node bilinear quadrilateral elements. A finer mesh at the contact region and a gradually coarser mesh further away from the contact surface were used to ensure the numerical accuracy and reduce the computational time. The boundary conditions are that the outer surface nodes were traction-free and the lower surface nodes were fixed. A numerical subroutine was implemented into ABAQUS that enables to assign individual constitutive properties to the element level. Convergence of the computations was checked by comparing the present results with those calculated using a finer mesh (elements), given virtually the same load-depth curve (as shown in the Fig. 2).

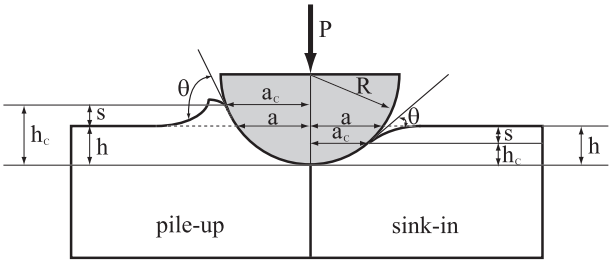

Fig. 3. Schematic diagram of contact geometry for normal spherical indentation.

3. Dimensional analysis

Dimensional analysis is a useful tool which has been widely used to analyze the indentation response and contact mechanics (Cheng and Cheng, 2004). In this section, we will apply the dimensional analysis to extract independent governing dimensionless parameters for load-depth curves and pile-up/sink-in behaviors in normal spherical indentation.

In normal indentation, the true contact area can be either underestimated/overestimated without considering pile-up/sink-in behaviors (Bolshakov and Pharr, 1998). The contact geometry for normal spherical indentation is illustrated in Fig. 3, which shows a rigid sphere of radius R driven into a material by a force P to a nominal indentation depth h. The left side of the figure shows the case of pile-up behavior, while right side of the figure shows the case of sink-in behavior. In the Fig. 3, h_C is the actual contact depth between the substrate and the rigid indenter, a is the surface contact radius defined by the intersection of the indenter with the original undeformed surface, a_C is the actual contact radius which is different from a because of pile up/sink in behavior, s is the height from the undeformed surface for pile-up or sink-in, the parameter θ is the angle between the tangent line to contact at its periphery and the undeformed surface. $s > 0$ corresponds to pile-up behavior, while $s < 0$ corresponds to sink-in behavior. The mean pressure (also called Meyer hardness) can be expressed as: $p_m = P/(\pi a_C^2)$.

For a normal spherical indentation into materials with PGSL, the load P and the pile-up/sink in behavior s depends on material properties and geometrical variables:

$$P = P(R, h, E^*, \sigma_{y,surf}, n_{surf}, h_{PGM}, \alpha) \tag{4}$$

$$s = s(R, h, E^*, \sigma_{y,surf}, n_{surf}, h_{PGM}, \alpha) \tag{5}$$

where R is the radius of the rigid sphere, h is the indentation depth, $E^* = E/(1 - \nu^2)$ is the reduced elastic modulus, $\sigma_{y,surf}$, n_{surf} are yield strength and strain hardening exponent of surface material respectively, h_{PGM} is the thickness of plastically graded layer, and α is the parameter of yield strength gradient.

Applying the Π theorem in dimensional analysis, the smallest number of independent variables can be obtained:

$$\frac{P}{E^*R^2} = \Pi_1\left(\frac{E^*}{\sigma_{y,surf}}, \frac{h}{R}, n_{surf}, \frac{h_{PGM}}{R}, \alpha R\right) \tag{6}$$

$$\frac{s}{h} = \Pi_2\left(\frac{E^*}{\sigma_{y,surf}}, \frac{h}{R}, n_{surf}, \frac{h_{PGM}}{R}, \alpha R\right) \tag{7}$$

where, $\frac{P}{E^*R^2}$, $\frac{s}{h}$ are dimensionless parameters for normalized load response and normalized pile-up/sink-in height respectively.

For homogeneous materials, Eqs. (6) and (7) are recovered to:

$$\frac{P}{E^*R^2} = \Pi_1\left(\frac{E^*}{\sigma_y}, \frac{h}{R}, n\right) \tag{8}$$

$$\frac{s}{h} = \Pi_2\left(\frac{E^*}{\sigma_y}, \frac{h}{R}, n\right) \tag{9}$$

For a given material property at the surface, Eqs. (6) and (7) can be reduced to:

$$\frac{P}{E^*R^2} = \Pi_1\left(\frac{h}{R}, \frac{h_{PGM}}{R}, \alpha R\right) \tag{10}$$

$$\frac{s}{h} = \Pi_2\left(\frac{h}{R}, \frac{h_{PGM}}{R}, \alpha R\right) \tag{11}$$

For spherical indentation on a PGSL (without gradients in elastic properties), there are three different deformation regimes: (a) initial pure elastic deformation: PGSL is no difference with homogeneous materials in this regimes and the indentation mechanics of PGSL should be the same as that of homogenous materials (Eqs. (8) and (9)); (b) the plastic zone is entirely within the graded layer: the indentation response should be independent of h_{PGM} and Eqs. (10) and (11) in this regime can be reduced to the following equations of (12) and (13); (c) the plastic zone goes beyond the PGSL: the indentation response of PGSL in this regime can be described by Eqs. (10) and (11).

$$\frac{P}{E^*R^2} = \Pi_1\left(\frac{h}{R}, \alpha R\right) \tag{12}$$

$$\frac{s}{h} = \Pi_2\left(\frac{h}{R}, \alpha R\right) \tag{13}$$

4. Results and discussions

4.1. Indentation mechanics for homogeneous materials

When the parameter of yield strength gradient is 0 ($\alpha = 0$), homogeneous materials are recovered. In this section, a parametric study was conducted to cover most common engineering materials, and both elastic and plastic responses (E^*/σ_y was varied from 44 to 1099, n was varied from 0 to 0.5, h/R was varied from 0 to 0.1, and Poisson ratio v was fixed at 0.3). In all simulations, the frictional coefficient was fixed at $\mu = 0.1$.

4.1.1. Background of elastic–plastic transition on indentation response

The loading response and pile-up/sink-in behaviors during the course of spherical indentation is strongly dependent on the relative amounts of elastic and plastic deformation. When the material is purely elastic ($E^*/\sigma_y = 0$), the sink in behavior can be well described by Hertzian contact theorey (Hertz, 1896). On the other hand, when the material is rigid-plastic ($E^*/\sigma_y = \infty$), the extensive pile up behavior has been well documented in the literature (Mattews, 1980; Hill et al., 1989; Biwa and Storakers, 1995; Taljat and Zacharia, 1998). It was found that influences of yield strength and indentation depth on the indentation response can be combined into one parameter that gives a unified description of the indentation behavior. This unified parameter is also found to be approximately equal to $2E^*h_C/(\sigma_y a_C)$ (Johnson, 1985; Taljat and Pharr, 2004), which can be calculated by the indentation depth and pile-up/sink-in parameter. Their work also showed that the indentation response converges very well when $2E^*h_C/(\sigma_y a_C)$ is used as the unified parameter describing both yield strength and indentation depth effects. So Eqs. (8) and (9) can be reduced to:

$$\frac{P}{\sigma_y \pi a_C^2} = \frac{p_m}{\sigma_y} = \Pi_1\left(\frac{2E^*h_C}{\sigma_y a_C}, n\right) \tag{14}$$

$$\frac{s}{h} = \Pi_2\left(\frac{2E^*h_C}{\sigma_y a_C}, n\right) \tag{15}$$

The influence of elastic–plastic transition on the indentation response for elastic-perfect plastic materials ($n = 0$) was given by the literature work (Taljat and Pharr, 2004). Our results obtained are in good agreement with Taljat's study (2004), so our figures are not repeated and only the main points are summarized here. The pile-up/sink-in parameter $\frac{s}{h}$ is -0.5 for purely elastic response, becomes positive with increasing of $2E^*h_C/(\sigma_y a_C)$, and finally reaches a plateau of 0.36 for fully plastic response. The normalized mean pressure (constrained factor) is consistent with Hertzian contact theory at small values of $2E^*h_C/(\sigma_y a_C)$, deviates from Hertzian contact theory at 2.5 of $2E^*h_C/(\sigma_y a_C)$, and finally reaches a plateau of 3 for fully plastic response.

4.1.2. Influence of two dimensionless parameters on indentation response

From last Section 4.1.1, it is shown that the spherical indentation response for homogeneous materials can be described only by two dimensionless parameters ($2E^*h_C/(\sigma_y a_C), n$). In this section, the effects of these two dimensionless parameters on indentation response are studied. Although preliminary results were presented in Taljat's study (2004), our work covered more common engineering materials and gave more detail results for both loading response and pile-up/sink-in behaviors. Fig. 4 shows the influences of both the unified parameter $2E^*h_C/(\sigma_y a_C)$ and strain hardening exponent n on the normalized pile-up/sink-in parameter. The results are composed of the unified behavior obtained for five different values of n ($n = 0, 0.1, 0.2, 0.3, 0.5$). Several interesting points are worthy of mention from Fig. 4. First, the pile-up/sink-in behavior is

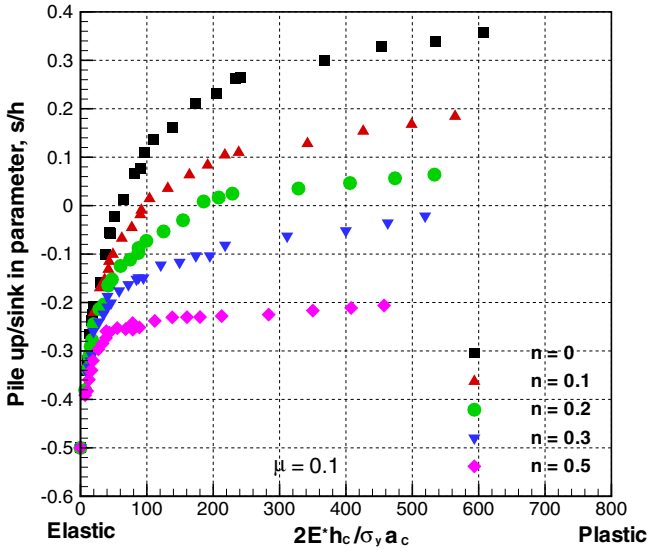

Fig. 4. The influences of both the unified parameter $2E^*h_C/(\sigma_y a_C)$ and strain hardening exponent n on the normalized pile-up/sink-in parameter.

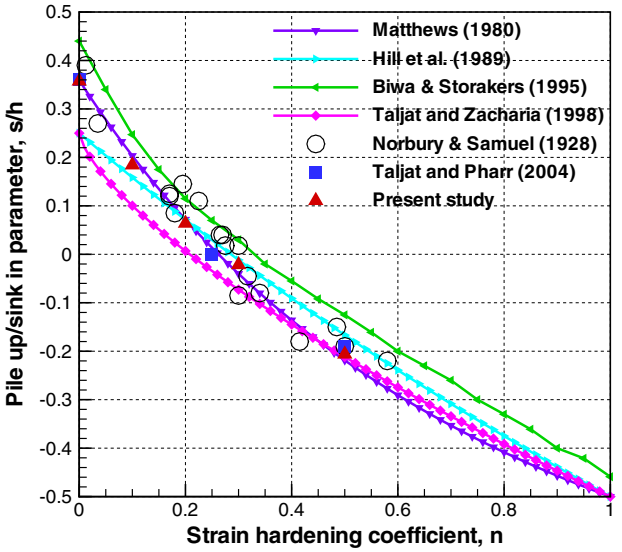

Fig. 5. The normalized pile-up/sink-in parameter s/h vs. strain hardening exponent n at fully plastic regime.

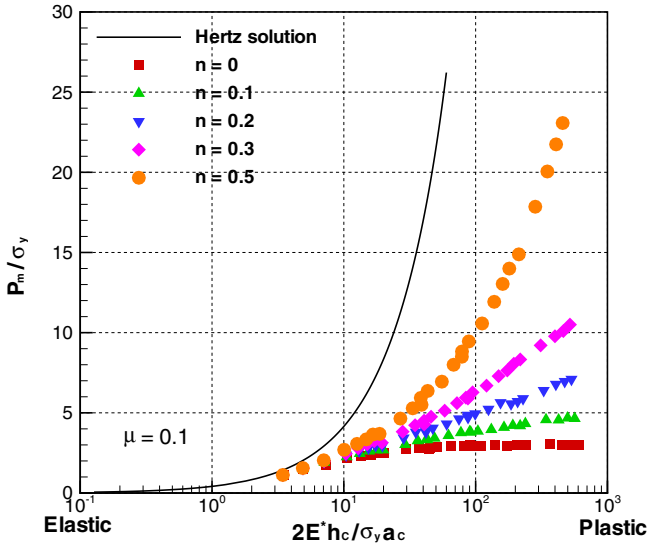

Fig. 6. The influences of both the unified parameter $2E^*h_C/(\sigma_y a_C)$ and strain hardening exponent n on the normalized mean pressure.

independent of strain hardening exponent at small values of $2E^*h_C/(\sigma_y a_C)$. This is because the material deforms only elastically at small values of $2E^*h_C/(\sigma_y a_C)$. Second, the pile-up/sink-in parameter grows larger with further increase of $2E^*h_C/(\sigma_y a_C)$ in a way that strongly depends on the strain hardening exponent. At the same value of $2E^*h_C/(\sigma_y a_C)$, larger s/h develops in material with smaller n. Third, the increase tendency of s/h slows down at large value of $2E^*h_C/(\sigma_y a_C)$, and finally reaches a nearly constant plateau at fully plastic regime. Fig. 5 shows the normalized pile-up/sink-in parameter s/h vs. strain hardening exponent n at fully plastic regime for the present study along with some data from the literature (Norbury and Samuel, 1928; Mattews, 1980; Hill et al., 1989; Biwa and Storakers, 1995; Taljat and Zacharia, 1998; Taljat and Pharr, 2004). It is shown that our results are in a good agreement with literature results, especially with Mattews' data (1980) and Taljat's data (Taljat and Pharr, 2004). Fig. 6 shows the influences of both the unified parameter $2E^*h_C/(\sigma_y a_C)$ and strain hardening exponent n on the normalized mean pressure. Several interesting points are also worthy of mention. First, the normalized mean pressure is independent of strain hardening exponent at small values of $2E^*h_C/(\sigma_y a_C)$. This is also because the plastic deformation of the material only commences at large value of $2E^*h_C/(\sigma_y a_C)$. Second, larger mean pressure develops in materials with larger n, and approaches the Herzian limit when $n = \infty$. Third, the condition of the constrained factor $p_m/\sigma_y = 3$ at fully plastic indentation stage is not valid any more for strain hardening materials. Fig. 6 can give a first estimate for the constrained factor at any indentation stage if the strain hardening exponent is known. From the combined results of Figs. 4 and 6, both elastic and plastic responses of spherical indentation for most common engineering materials (E^*/σ_y was varied from 44 to 1100, n was varied from 0 to 0.5, h/R was varied from 0 to 0.1) are quantitatively determined.

4.2. Indentation mechanics for materials with PGSL

Based on Eqs. (10) and (11), a parametric study of the effects of indentation depth, layer thickness of PGM and strength gradient parameter of PGM on normal spherical indentation deformation for materials with PGSL is presented in this section. The Young's modulus is fixed at 200 GPa, the Poisson ratio is fixed at 0.3, the strain hardening exponent is fixed at 0, and the radius of the rigid sphere is fixed at 0.5 mm. The yield strength for surface material is fixed at 1 GPa for a case study. The normalized PGM layer thickness h_{PGM}/R is varied from 0 to 0.4, the normalized indentation depth h/R is varied from 0 to 0.1, and the strength gradient parameter αR is varied from −4 to 4. These three dimensionless parameters cover a wide range of engineering applications for studying underlying indentation mechanisms for materials with PGSL.

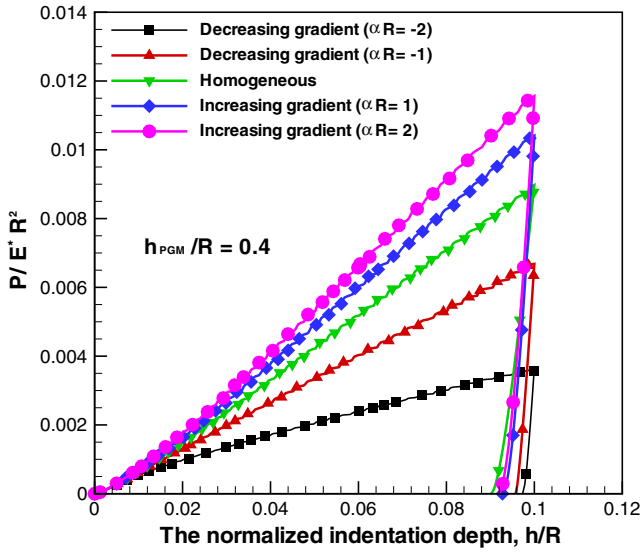

Fig. 7. The effect of strength gradient parameter on the normalized load response.

4.2.1. Influence of strength gradient parameter on indentation response

In order to study effect of strength gradient parameter on the indentation response only, the normalized PGM layer thickness h_{PGM}/R is fixed at 0.4, and the strength gradient parameter αR is varied from −2 to 2.

Fig. 7 shows the effect of strength gradient parameter on the normalized load response. In Fig. 7, two positive strength gradient cases $\alpha R = 1, 2$, two negative strength gradient cases $\alpha R = -1, -2$, and the case with the reference homogeneous material $\alpha R = 0$ are

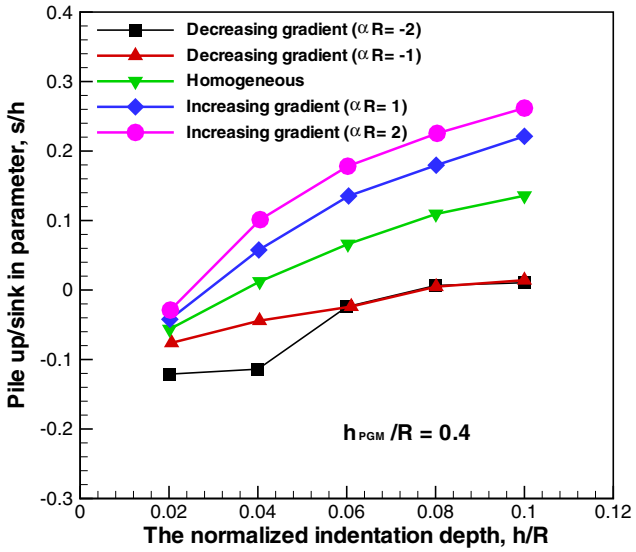

Fig. 8. The effect of strength gradient parameter on the normalized pile-up/sink-in parameter.

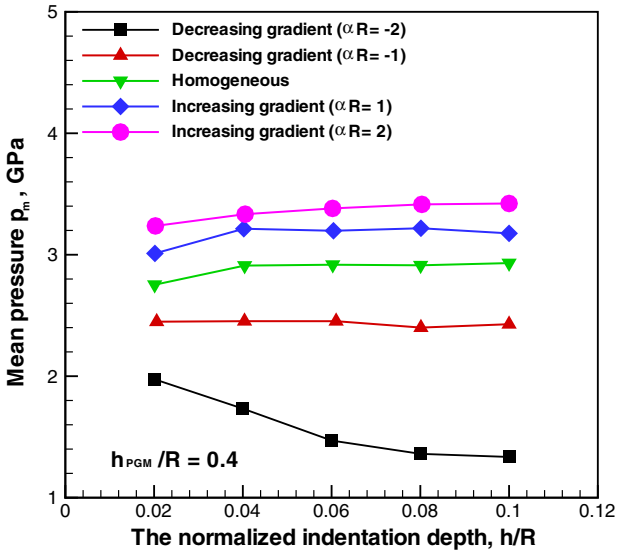

Fig. 9. The effect of strength gradient parameter on the mean pressure.

included. With the same surface properties as the reference homogeneous case, the negative (positive) gradient case bear less (more) load at the same indentation depth, as compared to the homogeneous case. Another important feature worthy of note is that the unloading behavior for each case is very similar. This is because the unloading behavior is only elastic response and independent of plastic properties and plastic gradients.

Fig. 8 shows the normalized pile-up/sink-in parameter vs. the normalized indentation depth for five different values of αR $(0,\pm1,\pm2)$. As expected, the normalized pile-up/sink-in parameter increases with the indentation depth for all cases, indicating that relative amount of plastic deformation is increasing along the indentation depth. Moreover, the normalized pile-up/sink-in parameter is found to be an increasing function of the strength gradient parameter of αR. Another interesting point is also worthy of mention. At large indentation depth ($h/R \geqslant 0.06$), the normalized pile-up/sink-in parameter reaches a limit ($s/h \approx 0$) and no longer decreases with further decreasing of αR for negative graded materials. For elastic-perfect plastic material ($n = 0$), the normalized pile-up/sink-in parameter increases significantly with increasing indentation depth. On the other hand, the normalized pile-up/sink-in parameter should decrease with increasing indentation depth because of negative gradient. These two competing factors reach a balance at large indentation depth ($h/R \geqslant 0.06$), so there is neither pile-up nor sink-in behavior for negative graded materials.

The influence of strength gradient parameter on mean pressure is shown in Fig. 9. The mean pressure is found to increase with increasing strength gradient parameter. Moreover, the mean pressure is found to be almost constant after certain indentation depth ($h/R \geqslant 0.04$) for homogeneous material and the graded materials with $\alpha R = \pm1, 2$, while it is not the case for the graded material with $\alpha R = -2$. The phenomenon for homogeneous case is consistent with the fact that the constrained factor reaches a plateau of 3 for fully plastic response as discussed in Section 4.1.1. The load P and the real contact area a_C both have higher (smaller) values for positive (negative) graded materials, as compared to those of homogeneous case at the same indentation depth. For $\alpha R = \pm1, 2$, these two competing factors reach a balance, so a plateau for mean pressure is observed. However, this balance is broken for $\alpha R = -2$ because of the unusual pile-up/sink-in behavior observed in Fig. 8.

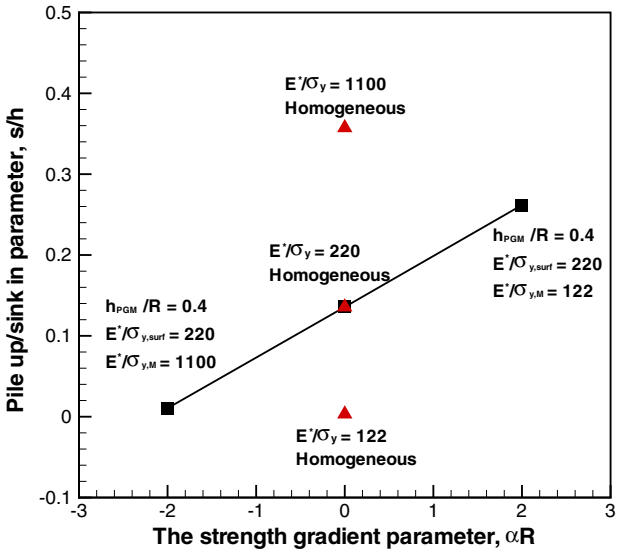

Fig. 10. The normalized pile-up/sink-in parameter vs. the strength gradient parameter at the normalized indentation depth of $h/R = 0.1$. Results for three homogeneous materials are also shown for comparison.

Fig. 10 shows the normalized pile-up/sink-in parameter vs. the strength gradient parameter at the normalized indentation depth of $h/R = 0.1$. The results for one positive gradient ($\alpha R = 2$) and one negative gradient ($\alpha R = -2$) are presented. For the positive gradient, the results for two homogeneous materials ($E^*/\sigma_{y,surf} = 220, E^*/\sigma_{y,M} = 122$) that constitute the bounding conditions for the graded layer are presented. For the negative gradient, the results for two homogeneous materials ($E^*/\sigma_{y,surf} = 220, E^*/\sigma_{y,M} = 1100$) that constitute the bounding conditions for the graded layer are also presented. In surprise, the normalized pile-up/sink-in parameter for the positive (negative) graded material is higher (lower) than that of both homogeneous surface material and homogeneous matrix material. For example, the positive graded material should be 'harder' than the homogeneous surface material with lowest yield strength ($E^*/\sigma_{y,M} = 220$) of the PGSL. One may think that the normalized pile-up/sink-in parameter for the homogeneous surface material ($E^*/\sigma_{y,M} = 220$) should be higher than that of the positive graded material, but it is not the case for the real results. These

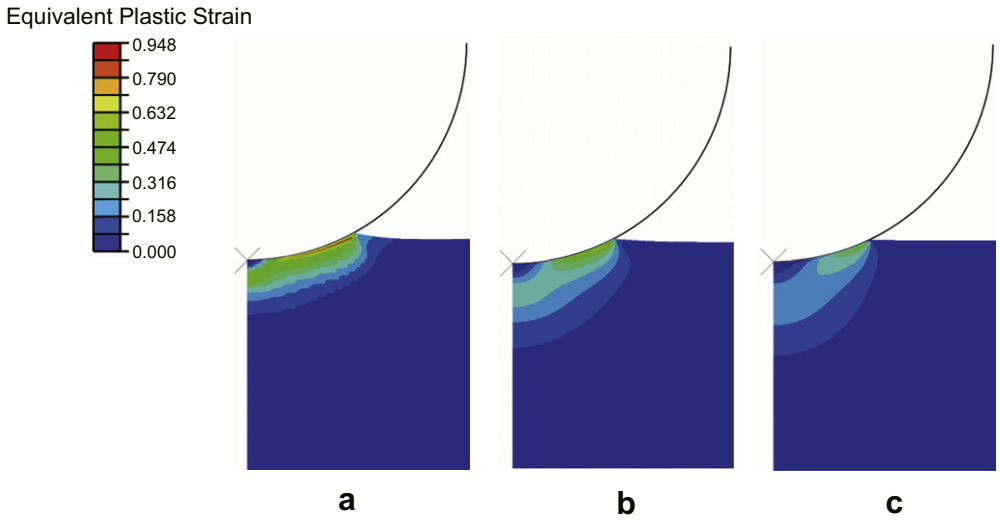

Fig. 11. Equivalent plastic strain contours for (a) positive gradient case ($\alpha R = 2, h_{PGM}/R = 0.4$), (b) homogeneous surface material with $E^*/\sigma_{y,surf} = 220$, (c) homogeneous matrix material with $E^*/\sigma_{y,M} = 122$.

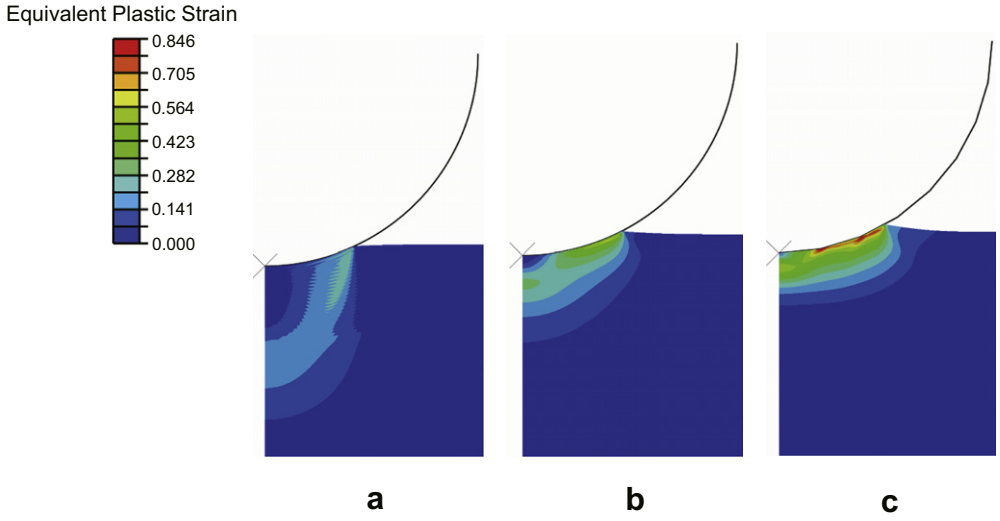

Fig. 12. Equivalent plastic strain contours for (a) negative gradient case ($\alpha R = -2, h_{PGM}/R = 0.4$), (b) homogeneous surface material with $E^*/\sigma_{y,surf} = 220$, (c) homogeneous matrix material with $E^*/\sigma_{y,M} = 1100$.

unexpected results are due to gradient effects, and will be further investigated and explained based on strain distribution maps in next paragraph. The plastic strain distribution under the indenter with and without plasticity gradient will be examined to rationalize the unusual trend.

Fig. 11 shows the equivalent plastic strain contours for positive gradient ($\alpha R = 2$) case and two homogeneous materials that constitute the bounding conditions for the graded layer. Fig. 12 shows the equivalent plastic strain contours for negative gradient ($\alpha R = -2$) case and two homogeneous materials that constitute the bounding conditions for the graded layer. For all cases shown in the figures, the normalized indentation depths are equal to 0.1. Under the same indentation depth, the maximum value of equivalent plastic strain is higher (lower) and the plastic zone size is smaller (larger) for the positive (negative) gradient material than those of both the homogeneous surface material and the homogeneous matrix material. Thus higher (lower) plastic strain accumulates near the indenter over a smaller (larger) plastic zone for the positive (negative) gradient case than those of two homogeneous cases. So, much higher (lower) equivalent plastic strain near the indenter pushes the materials upward (downward) during the indentation, resulting much higher (lower) pile-up value for the positive (negative) gradient case than those of two homogeneous cases. In summary, the positive (negative) strength gradient redistributes the plastic strain closer (farther) to the surface around the indentation impression, resulting in higher (lower) pile-up values.

During the contact and fatigue contact applications, cracks are formed mainly due to the maximum principal tensile stresses. So, the maximum principal tensile stress distribution maps for two negative gradient cases ($\alpha R = -2, -1$), the reference homogeneous case and two positive gradient cases ($\alpha R = 1, 2$) are compared at the same normalized indentation depth of 0.1 in Fig. 13. Under the same indentation depth, it is shown that the volume of tensile stress is larger (smaller) for the negative (positive) gradient case than the homogeneous case. Moreover, the surface area with tensile stress and the largest tensile stress increase with decreasing of αR. The results indicate that the positive plastically graded materials have significantly more resistance to contact crack formation.

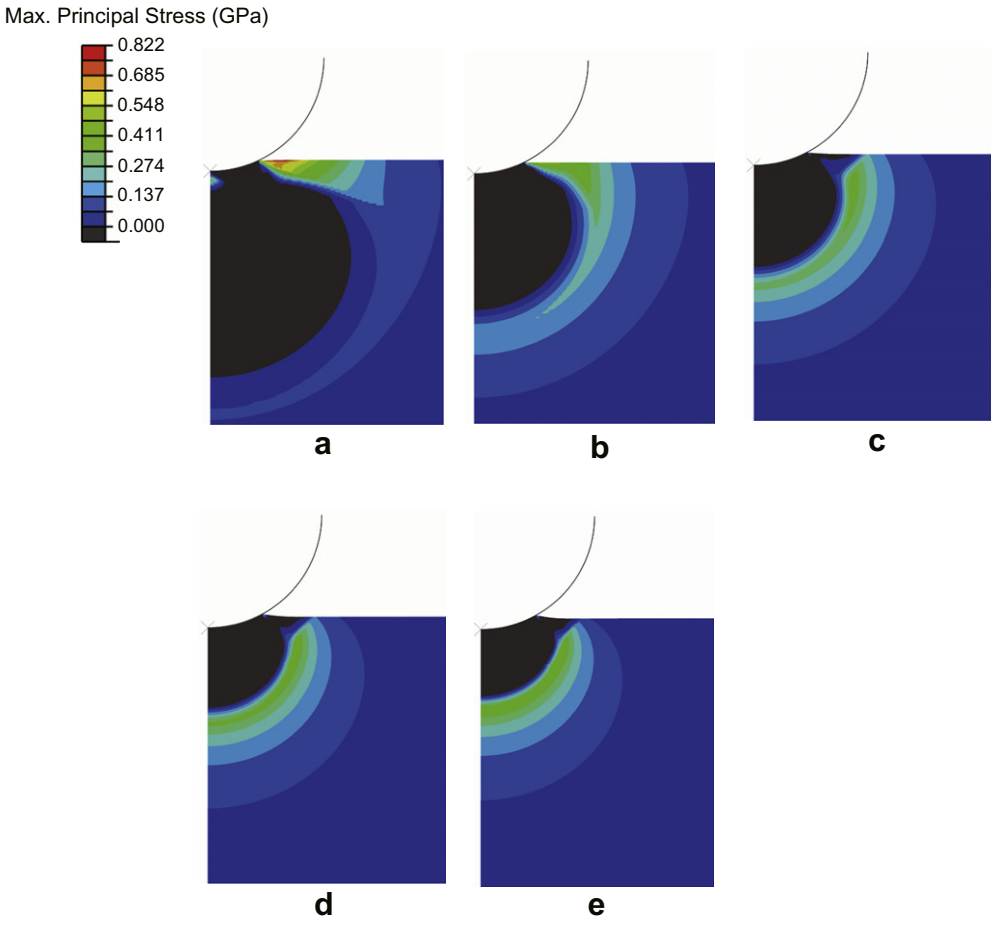

Fig. 13. Maximum principal tensile stress contours for (a) negative gradient case ($\alpha R = -2$), (b) negative gradient case ($\alpha R = -1$), (c) homogeneous surface material case, (d) positive gradient case ($\alpha R = 1$), (e) positive gradient case ($\alpha R = 2$).

4.2.2. Influence of thickness of PGSL on indentation response

In order to study effect of thickness of PGSL on the indentation response only, the strength gradient parameter αR is fixed at 2 for positive gradient and -2 for negative gradient. PGM layer thickness h_{PGM}/R is varied from 0 to 0.4.

Fig. 14 shows the effects of PGM layer thickness on the normalized load response for positive graded case ($\alpha R = 2$) and negative graded case ($\alpha R = -2$). Three different normalized PGM layer thickness ($h_{PGM}/R = 0, 0.2, 0.4$) are included for both positive and negative gradients. As shown, the normalized load is exactly the same value for different PGM layer thickness ($h_{PGM}/R = 0.2, 0.4$) when the normalized indentation depth is small ($h/R \leqslant 0.025$ for positive graded cases; $h/R \leqslant 0.01$ for negative graded cases). At this small indentation depth, the plastic zone is entirely within the graded layer for both cases ($h_{PGM}/R = 0.2, 0.4$), and the indentation response for PGSL should be independent of PGM layer thickness at this regime. However, the plastic zone goes beyond the graded layer at larger indentation depth ($h/R > 0.025$ for positive graded cases; $h/R > 0.01$ for negative graded cases), and the normalized load increases (decreases) with increasing PGM layer thickness for positive (negative) gradient cases. It is also interesting to note that the trend is not symmetric related to homogeneous material for positive and negative gradient cases. In general, the 'deformed plastic' zone becomes smaller (larger) when the materials of substrate become harder (softer) under the same indentation depth, which causes smaller (bigger) layer thickness effects for positive (negative) gradient cases.

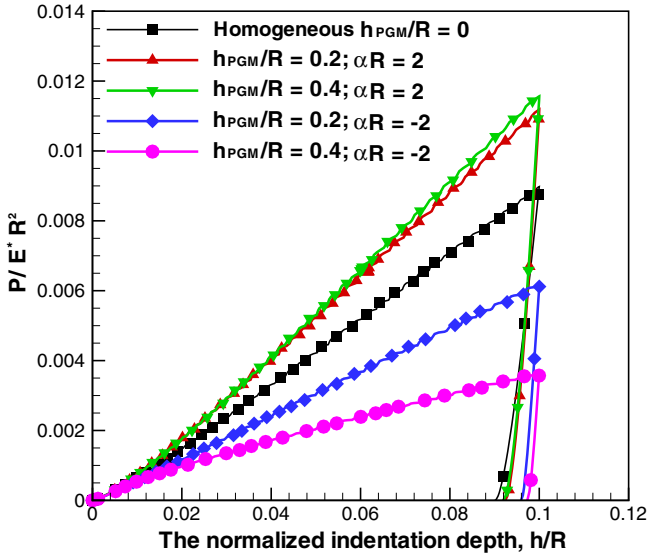

Fig. 14. The effect of PGM layer thickness on the normalized load response for positive gradient case of $\alpha R = 2$ and negative gradient case of $\alpha R = -2$.

Fig. 15 shows the effects of PGM layer thickness on the normalized pile-up/sink-in parameter for positive graded case ($\alpha R = 2$) and negative graded case ($\alpha R = -2$). As shown, the normalized pile-up/sink-in parameter is independent of PGM layer thickness

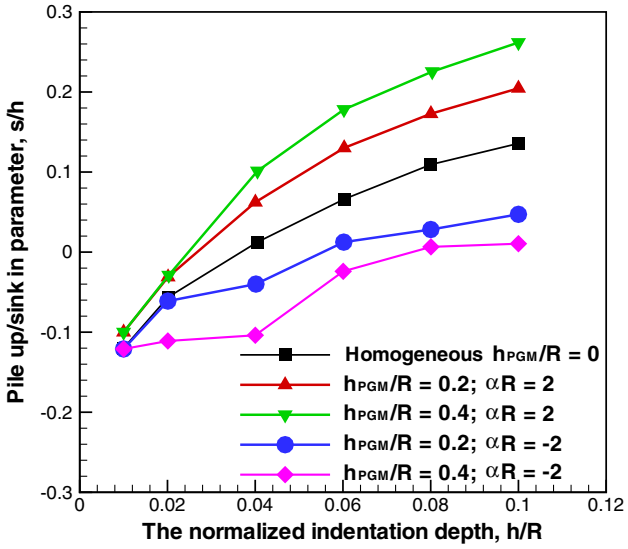

Fig. 15. The effect of PGM layer thickness on the normalized pile-up/sink-in parameter for positive gradient case of $\alpha R = 2$ and negative gradient case of $\alpha R = -2$.

when the normalized indentation depth is small ($h/R \leqslant 0.025$ for positive graded cases; $h/R \leqslant 0.01$ for negative graded cases). This is because the plastic zone is entirely within the graded layer at this regime. However, the normalized pile-up/sink-in parameter increases (decreases) with increasing PGM layer thickness for positive (negative) graded cases at larger indentation depth. The underlying mechanisms are very similar to those of Fig. 8. For positive (negative) graded materials, higher (lower) plastic strain accumulates near the indenter over a smaller (larger) plastic zone and results in higher (lower) pile-up values with the increasing PGM layer thickness.

5. Conclusions

In the present work, a comprehensive parametric study for establishing contact mechanics of instrumented normal spherical indentation on homogeneous materials and materials with plastically graded surface layer is presented. The important concluding remarks are summarized as follows:

1. Based on dimensional analysis and literature work (Johnson, 1985; Taljat and Pharr, 2004), the dependencies of indentation response for homogeneous materials can be described only by two dimensionless parameters: $2E^*h_C/(\sigma_y a_C)$ and n. The results presented in the present study may be used as a first estimate of loading response and pile-up/sink-in behavior when the material parameters are known. These results also can help to determine the real contact area during the load and depth sensing indentation if one has some idea of the material parameters of E^*/σ_y and n.
2. For a fixed surface material, the indentation response for materials with PGSL can be described only by three dimensionless parameters: the normalized indentation depth h/R, the normalized PGM layer thickness h_{PGM}/R, and the dimensionless strength gradient parameter αR. The results show that the materials can bear more load with larger strength gradient parameter for a fixed PGM layer thickness and a given indentation depth. At large indentation depth, the normalized load increases (decreases) with increasing PGM layer thickness for a fixed positive (negative) gradient case. Moreover, the normalized pile-up/sink-in parameter is found to be an increasing function of the strength gradient parameter of αR, and increases (decreases) with increasing PGM layer thickness for a fixed positive (negative) gradient parameter at large indentation depth.
3. The normalized pile-up/sink-in parameters for materials with positive (negative) graded layer are higher (lower) than those of both homogeneous surface material and homogeneous matrix material that constitute the bounding conditions for the graded layer. These non-intuitive results are explained by the plastic strain distributions under the indenter impression. The positive (negative) strength gradient redistributes the plastic strain closer (farther) to the surface around the indentation impression, resulting in higher (lower) pile-up values.
4. Under the same indentation depth, it is shown that the volume of maximum tensile stress is smaller (larger) for the positive (negative) gradient case than the homogeneous case. Moreover, the surface area with tensile stress and the largest maximum tensile stress decrease with increasing of strength gradient parameter. The results indicate that the materials with positive PGM layer have significantly more resistance to contact crack formation.

Acknowledgements

The authors would like to acknowledge the financial support of NSFC (Grants Nos. 11002151 and 11072243), 973 Project of China (No. 2010CB631004) and Knowledge Innovation Program of Chinese Academy of Sciences (No. KJCX2-EW-L03).

References

ABAQUS Theory Manual (v6.8), 2008. SIMULIA Corp., Providence, RI, USA.
Bartier, O., Hernot, X., Mauvoisin, G., 2010. Theoretical and experimental analysis of contact radius for spherical indentation. Mech. Mater. 42, 640–656.
Biwa, S., Storakers, B., 1995. An analysis of fully plastic Brinell indentation. J. Mech. Phys. Solids 43 (8), 1303–1333.
Bolshakov, A., Pharr, G.M., 1998. Influences of pileup on the measurement of mechanical properties by load and depth sensing indentation techniques. J. Mater. Res. 13 (4), 1049–1058.
Branch, N.A., Arakere, N.K., Subhash, G., Klecha, M.A., 2011. Determination of constitutive response of plastically graded materials. Int. J. Plastic. 27, 728–738.
Cao, Y.P., Lu, J., 2004a. A new method to extract the plastic properties of metal materials from an instrumented spherical indentation loading curve. Acta Mater. 52, 4023–4032.
Cao, Y.P., Lu, J., 2004b. A new scheme for computational modeling of conical indentation in plastically graded materials. J. Mater. Res. 19 (6), 1703–1716.
Chen, X.H., Lu, J., Lu, L., Lu, K., 2005. Tensile properties of a nanocrystalline 316L austenitic stainless steel. Scripta Mater. 52, 1039–1044.
Cheng, Y.T., Cheng, C.M., 2004. Scaling, dimensional analysis, and indentation measurements. Mat. Sci. Eng. R 44 (4-5), 91–149.
Cheng, Y.T., Page, T., Pharr, G.M., Swain, M.V., Wahl, K.J.E., 2004. Special focus issue: fundamentals and applications of instrumented indentation in multidisciplinary research. J. Mater. Res. 19 (1), 1–2.
Choi, I.S., Detor, A.J., Schwaiger, R., Dao, M., Schuh, C.A., Suresh, S., 2008a. Mechanics of indentation of plastically graded materials – II: experiments on nanocrystalline alloys with grain size gradients. J. Mech. Phys. Solids 56, 172–183.
Choi, I.S., Dao, M., Suresh, S., 2008b. Mechanics of indentation of plastically graded materials – I: analysis. J. Mech. Phys. Solids 56, 157–171.
Dao, M., Lu, L., Asaro, R.J., De Hosson, J.T.M., Ma, E., 2007. Toward a quantitative understanding of mechanical behavior of nanocrystalline metals. Acta Mater. 55, 4041–4065.
Giannakopoulos, A.E., Suresh, S., 1997. Indentation of solids with gradients in elastic properties. 2. Axisymmeric indenters. Int. J. Solids Struct. 34 (19), 2393–2428.
Giannakopoulos, A.E., 2002. Indentation of plastically graded substrates by sharp indentors. Int. J. Solids Struct. 39, 2495–2515.
Gouldstone, A., Chollacoop, N., Dao, M., Li, J., Minor, A.M., Shen, Y.-L., 2007. Overview: indentation across size scales and disciplines: recent developments in experimentation and modeling. Acta Mater. 55 (12), 4015–4039.
Habbab, H., Mellor, B.G., Syngellakis, S., 2006. Post-yield characterization of metals with significant pile-up through spherical indentations. Acta Mater. 54, 1965–1973.
Hernot, X., Bartier, O., Bekouche, Y., Abdi, R.El., Mauvoisin, G., 2006. Influence of penetration depth and mechanical properties on contact radius determination for spherical indentation. Int. J. Solids Struct. 43, 4136–4153.

Hertz, H. 1896. Miscellaneous Papers by H. Hertz Macmillan, London.
Hill, R., Storakers, B., Zdunek, A.B., 1989. A theoretical study of the Brinell hardness test. Proc. Roy. Soc. Lond. A 423, 301–330.
Jitcharoen, J., Padture, N.P., Giannakopoulos, A.E., Suresh, S., 1998. Hertzian-crack suppression in ceramics with elastic-modulus-graded surfaces. J. Am. Ceram. Soc. 81 (9), 2301–2308.
Johnson, K.L., 1985. Contact Mechanics. Cambridge University Press, Cambridge, UK.
Kim, S.H., Lee, B.W., Choi, Y., Kwon, D., 2006. Quantitative determination of contact depth during spherical indentation of metallic materials – a FEM study. Mat. Sci. Eng. A Struct. 415, 59–65.
Kogut, L., Komvopoulos, K., 2004. Analysis of the spherical indentation cycle for elastic-perfectly plastic solids. J. Mater. Res. 19 (12), 3641–3653.
Lee, H., Lee, J.H., Pharr, G.M., 2005. A numerical approach to spherical indentation techniques for material property evaluation. J. Mech. Phys. Solids 53, 2037–2069.
Mattews, J.R., 1980. Indentation hardness and hot pressing. Acta Metal. 28, 311–318.
Meyers, M.A., Mishra, A., Benson, D.J., 2006. Mechanical properties of nanocrystalline materials. Prog. Mater. Sci. 51, 427–556.
Nakamura, T., Wang, T., Sampath, S., 2000. Determination of properties of graded materials by inverse analysis and instrumented indentation. Acta Mater. 48, 4293–4306.
Nastasi, M., Mayer, J.W., Hirvonen, J.K., 1998. Ion-Solid Interactions: Fundamentals and Applications. Cambridge University Press, Cambridge, UK.
Norbury, A.L., Samuel, T., 1928. The recovery and sinking-in or piling-up of material in the Brinell test, and the effect of these factors on the correlation of the Brinell with other hardness tests. J. Iron Steel I. 117, 673–687.
Roland, T., Retraint, D., Lu, K., Lu, J., 2006. Fatigue life improvement through surface nanostructuring of stainless steel by means of surface mechanical attrition treatment. Scripta Mater. 54, 1949–1954.
Roland, T., Retraint, D., Lu, K., Lu, J., 2007. Enhanced mechanical behavior of a nanocrystallised stainless steel and its thermal stability. Mat. Sci. Eng. A Struct., 281–288.
Suresh, S., Mortensen, A. 1998. Fundamentals of Functionally Graded Materials. Institute of Materials, London.
Suresh, S., Olsson, M., Giannakopoulos, A.E., Padture, N.P., Jitcharoen, J., 1999. Engineering the resistance to sliding-contact damage through controlled gradients in elastic properties at contact surfaces. Acta Mater. 47 (14), 3915–3926.
Suresh, S., 2001. Graded materials for resistance to contact deformation and damage. Science 292, 2447–2451.
Taljat, B., Zacharia, T., 1998. New analytical procedure to determine stress-strain curve from spherical indentation data. Int. J. Solids Struct. 35, 4411–4426.
Taljat, B., Pharr, G.M., 2004. Development of pile-up during spherical indentation of elastic-plastic solids. Int. J. Solids Struct. 41, 3891–3904.
Tao, N.R., Wang, Z.B., Tong, W.P., Sui, M.L., Lu, J., Lu, K., 2002. An investigation of surface nanocrystallization mechanism in Fe induced by surface mechanical attrition treatment. Acta Mater. 50, 4603–4616.
Tartaglia, J.M., Eldis, G.T., 1984. Core hardenability calculations for carburizing steels. Metall. Trans. 15, 1173–1183.
Vanlandingham, M.R., 2003. Review of instrumented indentation. J. Res. Natl. Inst. Stan. Tech. 108 (4), 249–265.
Waltz, L., Retraint, D., Roos, A., Olier, P., 2009. Combination of surface nanocrystallization and co-rolling: creating multilayer nanocrystalline composites. Scrip. Mater. 60, 21–24.